Generation of >3 μm high peak power Raman soliton exceeding 2 MW in 10 centimeters large core fluorotellurite fiber

Linjing Yang[1], Chuanfei Yao[1]*, Xuan Wang[1], Kaihang Li[1], Guochuan Ren[1], Luyao Pu[1], and Pingxue Li[1]*

[1]*State Key Laboratory of Materials Low-Carbon Recycling, Beijing University of Technology, Beijing 100124, China*

**Correspondence:*

yaochuanfei@bjut.edu.cn;

pxli@bjut.edu.cn

Abstract

In this work, we demonstrate the generation of high-performance tunable Raman solitons beyond 3 μm in a 10 centimeters, large core (40 μm) fluorotellurite fiber. The pump source is a high-peak-power Raman soliton generated through soliton fission in a silica fiber. By further cascading the 10 cm highly nonlinear fluorotellurite fiber, this Raman soliton undergoes successive high-order soliton fission and soliton self-frequency shift with a tunable range of 2.7-3.3 μm. Such an ultra-short length and ultra-large core fiber significantly reduce the pulsewidth of the 3.3 μm Raman soliton to 55 fs, doubling the peak power to 2.3 MW compared to previous studies. Furthermore, owing to the seed's high-repetition-frequency feature, the 3.3 μm Raman soliton's power exceeds 2 W. These performance metrics represent the highest levels achieved for Raman solitons at wavelengths above 3 μm, offering a simple and effective new approach for generating high-peak-power femtosecond pulses in the mid-infrared spectral region.

Key words: *mid-infrared femtosecond laser; Raman soliton; fluorotellurite fiber; high peak power*

1. Introduction

High-power, high-peak-power mid-infrared (MIR) femtosecond laser sources around 3 μm hold significant application value in fields such as strong-field physics[1,2], polymer material processing[3,4], ultrafast spectroscopy[5,6], and biomedical science[7]. Among the various methods for generating femtosecond laser in this wavelength range, soliton self-frequency shift (SSFS) in nonlinear MIR fibers is one of the most effective approaches[8,9]. Traditional implementations of this method place great emphasis on using fibers with low nonlinear coefficients and long

10.1017/hpl.2025.10042

fiber lengths as the nonlinear frequency-shifting medium. A lower nonlinear coefficient effectively reduces the soliton order of the input pulse, thereby preventing the formation of multiple higher-order Raman solitons and ensuring a higher energy ratio of the first fundamental Raman soliton. However, the low nonlinearity coefficient also reduces the frequency shift of the Raman soliton, necessitating longer fiber lengths and smaller core diameters to compensate for the insufficient frequency shift. The most representative MIR fiber that meets these criteria is fluoride fiber, particularly ZBLAN fiber, which has been extensively studied for generating tunable MIR Raman solitons[10-13]. In 2022, Ren et al. demonstrated a high-power, tunable femtosecond laser based on polarization control in a 12 m ZBLAN fiber. The central wavelength of the MIR Raman soliton could be tuned from 1.96 μm to 3.1 μm, its maximum average power exceeded 350 mW, with a peak power of only 0.06 MW and a pulse energy of less than 10 nJ[14]. To mitigate the impact of excessive fiber length on pulsewidth and peak power, Tiliouine et al. employed a 3.5 m large mode area (LMA) (26 μm) fluoride fiber as a nonlinear frequency-shifting medium to generate high-performance MIR Raman solitons beyond 3 μm. The furthest Raman soliton, centered at 3.17 μm, exhibited a pulsewidth of 165 fs and a peak power of approximately 0.28 MW[15]. Recently, our research group has also investigated the generation of high-energy, high-peak-power Raman solitons in ZBLAN fiber. By coupling a 976 nm pump laser into a 3 m Er^{3+}-doped ZBLAN fiber for Raman soliton amplification, we achieved tunable femtosecond pulses spanning 2.1–3.5 μm. The maximum Raman soliton energy reached 107 nJ, with a peak power as high as 0.82 MW, representing the highest peak power Raman soliton ever reported in fluoride fiber[16]. These results indicate that although ZBLAN fiber could enable the generation of tunable femtosecond pulses beyond 3 μm, and both peak power and pulse energy have been improved to some extent through fiber length reduction, core size enlargement, or gain-modulation, the utilization of meter-scale fibers still leads to extended Raman soliton propagation distance and increased dispersion effect. Consequently, the relatively wide pulsewidths (>100 fs) limit further breakthroughs in higher peak power (MW level).

Contrary to the conventional understanding of Raman soliton generation, we propose that short-length, high-nonlinearity mid-infrared fiber media are the optimal choices for enhancing the performance of MIR Raman solitons, such as tellurite fibers[17-19]. A few studies have already demonstrated the feasibility of generating Raman solitons in these fibers. For instance, Li et al. used a 0.5 m all-solid fluorotellurite fiber with a core diameter of 2.7 μm as the nonlinear medium to generate tunable MIR Raman solitons in the range of 1.96–2.82 μm, with an output power of 90 mW and a peak power of 0.016 MW[20]. Chang et al. used a 2.8 μm Er^{3+}: ZBLAN fiber amplifier to pump a 21 cm fluorotellurite fiber with a 5 μm core diameter, achieving a maximum redshifted Raman soliton wavelength of 3.17 μm, with an output power of 39 mW and a peak power of only 0.007 MW[21]. Although these studies utilized relatively short fiber lengths, the small core diameters of the fluorotellurite fibers limited the achievable

https://doi.org/10.1017/hpl.2025.10042 Published online by Cambridge University Press

energy and peak power of the Raman solitons, resulting in a significant performance gap compared to traditional fluoride fibers. Recently, our research group employed a custom-fabricated fluorotellurite fiber with a 30 μm core diameter and a length of approximately 35 cm as the nonlinear frequency-shifting medium. Under high-peak-power pumping, we achieved MIR Raman solitons with an output power exceeding 1 W and peak power reaching the MW level[22]. However, a limitation of this work was that the pump source and the fluorotellurite fiber were mechanically spliced, leading to poor coupling efficiency and stability.

In this work, we overcome the challenges of fusion splicing between LMA fluorotellurite fibers and silica fibers, significantly enhancing the coupling efficiency of the pump laser into the fluorotellurite fiber. By using a larger core diameter of 40 μm and a fiber length of 10 cm fluorotellurite fiber, we greatly improve the output performance of MIR Raman solitons, which can be frequency-shifted up to 3.3 μm under the pumping of a 2.27 μm high-peak-power Raman soliton source. The output power and peak power of the soliton were 2.1 W and 2.3 MW, respectively, demonstrating the powerful capability of ultrashort-length fluorotellurite fibers for generating tunable MIR femtosecond pulses.

2. Experimental setup

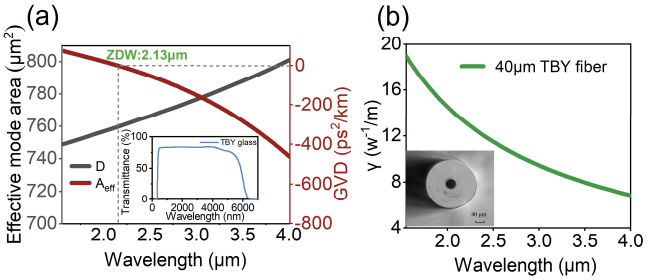

Figure 1. (a) Variation of group-velocity dispersion (GVD) and effective mode area and (b) nonlinear Kerr coefficient (γ) of 40 μm fluorotellurite fibers with wavelength, with the inset showing the Transmission spectrum curve of TBY glass

Firstly, we fabricated an all-solid fluorotellurite (TBY) fiber with a core diameter of 40 μm using the rod-in-tube method. The core and cladding materials were composed of $70TeO_2$-$20BaF_2$-$10Y_2O_3$ and $60TeO_2$-$25BaF_2$-$10Y_2O_3$, respectively. The numerical aperture (NA) of the fiber at 2 μm is approximately 0.5. As shown in the inset of Figure 1(a), we measured the transmittance curve of the TBY glass. It can be observed that the material loss of TBY glass exhibits a transmission window covering 0.4-6.0 μm, with no significant -OH absorption peaks observed in the spectrum, indicating an extremely low -OH content in the glass system.

The dispersion and mode area curves of the fiber between 1.5 μm and 4 μm were calculated using the full-vector finite difference method, as shown in Figure 1(a). The zero dispersion point is located at 2.13 μm. As the wavelength increases, the anomalous dispersion value of the LMA fluorotellurite fiber continuously increases, while the mode area increases from 748.6 μm² to 800.9 μm². The corresponding nonlinear coefficient decreases from 0.0019 W^{-1}/m to 0.00068 W^{-1}/m. Additionally, the transmission loss of the fiber at 2 μm was measured using the

https://doi.org/10.1017/hpl.2025.10042 Published online by Cambridge University Press

cut-back method and was calculated to be approximately 0.3 dB/m. According to the equation [23].

$$E_P = \frac{2|\beta_2|}{|\gamma|T_0}, \tag{1}$$

with β_2 the group velocity dispersion (GVD) of fiber, T_0 the pulse duration, γ the nonlinear coefficient of the fiber which is defined as

$$\gamma = \frac{n_2\omega_0}{cA_{eff}} \tag{2}$$

with n_2 the nonlinear refractive index of the fiber and A_{eff} the effective mode area. Based on the fluorotellurite fiber's parameters, a larger mode area corresponds to a larger soliton area, which will significantly enhance the energy of the fundamental Raman solitons generated in the fiber. Furthermore, the soliton frequency shift distance Ω can be defined as:

$$\Omega = -\frac{8T_R\gamma P_0}{15T_0^2}z \tag{3}$$

with P_0 is the peak power, z the fiber length, T_R is the first moment of the nonlinear response function. From this equation, a high nonlinear coefficient (an order of magnitude higher than that of conventional fluoride fibers) will ensure that Raman solitons can shift to longer wavelengths within a shorter TBY fiber length.

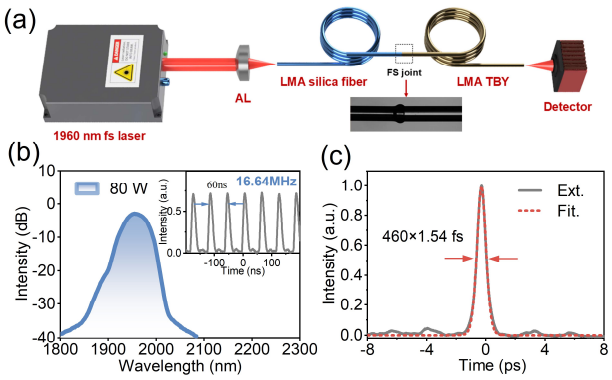

Figure 2. (a) The experimental setup for high-power Raman soliton frequency shift in a cascade-pumped fluorotellurite fiber (AL: aspherical lens); (b) the pulse spectrum (with the inset of sequence of seed laser) at 80W pump power; (c) the pulsewidth after the compressor at 80W pump power.

Figure 2(a) shows the experimental setup of high power MIR tunable femtosecond laser, consisting of a 1960 nm femtosecond laser, an aspheric lens, an LMA silica fiber, and an LMA TBY fiber. The 1960 nm femtosecond laser is a self-made chirped pulse amplification (CPA) system with a repetition frequency of 16.64 MHz. We also characterized the CPA system's spectrum and pulse width (460 fs) at a pump power of 80 W, as shown in Figure 2 (b) and (c). The autocorrelation trace exhibits a negligible pedestal, indicating the absence of significant nonlinear effects in the amplifier. Specific parameters can be found in our previous work[22]. Considering that directly pumping the TBY fiber in its normal dispersion region would delay

https://doi.org/10.1017/hpl.2025.10042 Published online by Cambridge University Press

the excitation of higher-order soliton fission and SSFS, leading to relatively poor frequency shift effect, we first use a 50 mm aspheric lens to couple the femtosecond laser into LMA silica fiber. The coupling efficiency at low pump power can exceed 70%. According to our previous calculations[24], the zero-dispersion point of this fiber is <1500 nm, allowing the Raman soliton that cross the zero-dispersion point of TBY fiber in the LMA silica fiber. Unlike the mechanical splicing of the LMA silica fiber and LMA TBY fiber in the previous experimental setup, here we explored the fusion splicing process between the two fibers. The fusion result is shown in the inset of Figure 2, where the silica fiber has a size of 32/250 μm, and the TBY fiber has a size of 40/250 μm. The splicing efficiency could reach 84% (considering Fresnel reflection), which improves the overall stability of the system. The lengths of the silica fiber and TBY fiber used in the experiment are 27 cm and 10 cm, respectively. Compared to the traditional multi-meter-long fluoride fibers, the ultrashort length of the TBY fiber greatly saves system space and allows for more convenient thermal management. Throughout the experiment, the output spectrum from both the LMA silica fiber and the TBY fiber was measured using a monochromator equipped with a mercury cadmium telluride (MCT) detector.

3. Results and discussion

In the experiment, a commercially available 32/250 LMA silica fiber is employed as a transitional medium to enhance the pulse peak power. We first characterized the mode field area, group-velocity dispersion (GVD), and nonlinear coefficient of this fiber. As shown in Figure 3(a), the fiber exhibits anomalous dispersion across the entire 1.9-2.4 μm range, with a dispersion value of -76 ps²/km at the pump center wavelength (1960 nm). The presence of anomalous dispersion is favorable for the excitation of self-phase modulation (SPM) and the SSFS. Figure 3(b) illustrates the variation of the nonlinear coefficient, the overall nonlinear coefficient is approximately one order of magnitude lower than that of fluorotellurite fibers.

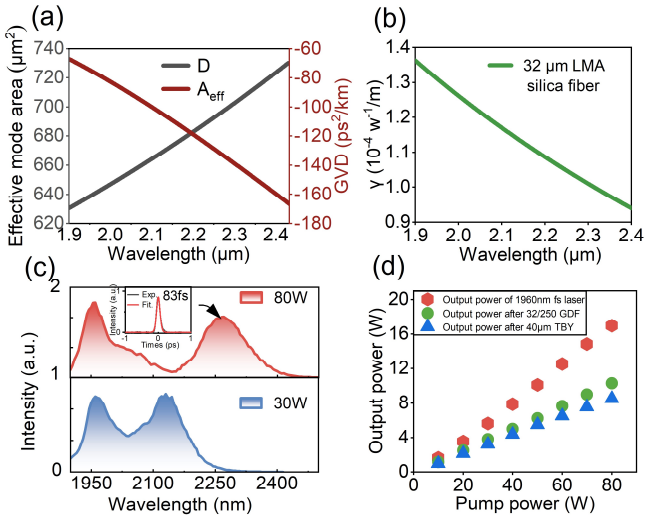

Figure 3. Variation of (a) GVD, effective mode area and (b) nonlinear Kerr coefficient (γ) of 32/250 silica fiber, (c) Variation of the frequency shift spectrum of the Raman soliton in LMA silica fiber at 30W,

https://doi.org/10.1017/hpl.2025.10042 Published online by Cambridge University Press

80W pump power, with the inset showing the autocorrelation trace of Raman soliton at a pump power of 80 W; (d) Variation of the output power of the1960 nm femtosecond laser, 32/250 silica fiber and 40 μm TBY fiber as a function of pump power

As shown in Figure 3(c), at a pump power of 80 W, the center wavelength of the Raman soliton can be shifted to 2270 nm. By using the unchirped, narrow-pulsewidth Raman soliton to pump the TBY fiber in its anomalous dispersion region, the SPM and SSFS effects will be rapidly excited. On the other hand, according to Figure 3(c), the Raman soliton spectrum generated in the silica fiber contains significant residual pump light components. The zero-dispersion point at 2.13 μm can attenuate the SPM of the residual signal light, preventing excessive spectral components from entering the anomalous dispersion region, thereby enhancing the purity of the entire Raman soliton frequency-shifted spectrum. As shown in Figure 3(d), the output power after the 1960 nm femtosecond laser, the silica fiber, and the TBY fiber reaches 17 W, 10.31 W, and 8.5 W at a 80 W pump power of 793 nm. The Raman soliton's power at 2.27 μm reaches 4.75 W, with a corresponding pulse energy of 285 nJ and a pulsewidth of only 83 fs. According to equation (2), such a narrow pulsewidth will further increase the frequency shift of the Raman soliton towards longer wavelengths in the TBY fiber.

Subsequently, we investigated the SSFS in a 10 cm TBY fiber, leveraging its high nonlinearity coefficient to compensate for the short length limitation. As shown in Figure 4(a), under a pump power of 30 W, a Raman soliton was directly generated at 2.7 μm within the TBY fiber. This demonstrates the high nonlinearity coefficient of the TBY fiber. As shown in Figure 3(c), the center wavelength of the Raman soliton split from the silica fiber had just crossed the zero-dispersion wavelength of the TBY fiber, it will evolve into a high-order soliton state upon entering the TBY fiber. According to the soliton order N calculation equation,

$$N^2 = \frac{|\gamma| P_0 T_0^2}{2|\beta_2|} \tag{4}$$

the dispersion at 2.3 μm for TBY fiber is -23 ps²/km, the nonlinear coefficient γ is 0.00125 W^{-1}/m, the measured T_{FWHM} is approximately 83 fs (with $T_0 = T_{FWHM}/1.76$), and the peak power is about 3.43 MW. Based on the above values, the soliton order of the Raman soliton is calculated to be $N = 15.1$. Such a high-order soliton pulse will experience intense SPM effects after entering the TBY fiber, causing the spectrum to rapidly broaden and leading to higher-order soliton fission again. Under the influence of Raman scattering within the pulse, the Raman soliton quickly shifts to 2.7 μm. As the pump power of the 1960 nm femtosecond laser increases from 30 W to 80 W, the frequency shift speed of the Raman soliton begins to slow down at 60 W. Between 60 W and 80 W, it only shifts by 70 nm. There are two main reasons for this: first, the Raman soliton generated in the pre-stage (silica fiber) has already located in the high-loss region of the silica material, and its energy and peak power tend to saturate, which in turn slows down the frequency shift in the TBY fiber. Second, the length of the fiber is relatively short, limiting the further frequency shift of the Raman soliton. Nevertheless, the Raman soliton still

https://doi.org/10.1017/hpl.2025.10042 Published online by Cambridge University Press

shifts to >3 μm and can ultimately reach up to 3.3 μm.

On the other hand, we also attempted to directly couple the compressed laser pulse into the 10 cm TBY fiber with 40 μm core diameter at the 8.5 W output power, which corresponds to the case where the pump power (793 nm) was 80 W when LMA silica fiber was added as a transitional fiber. When directly pumping the TBY fiber, the input pulsewidth was 460 fs, the output power was 8.5 W, and the peak power was 1.1 MW. This yields a corresponding soliton order of approximately 45(As calculated from Equation (4)), meaning that more fundamental soliton pulses will be split in TBY fiber. It is easy to form a supercontinuum rather than a single Raman soliton, as shown in the inset of Figure 4(a). Additionally, according to Equation (3), the frequency shift distance is inversely proportional to the square of the pulsewidth and directly proportional to the peak power. Since the peak power in the direct pumping case is lower than that of the 2.3 μm Raman soliton generated by the silica fiber, and the pulsewidth is larger, the frequency shift distance of the first-order Raman soliton responsible for spectral broadening is also much smaller than in the case of adding silica fiber as a transitional fiber. Therefore, the spectral edge only shifts to around 3 μm when directly pumping the TBY fiber, it is necessary to add silica fiber as a transitional fiber for the formation of the Raman soliton.

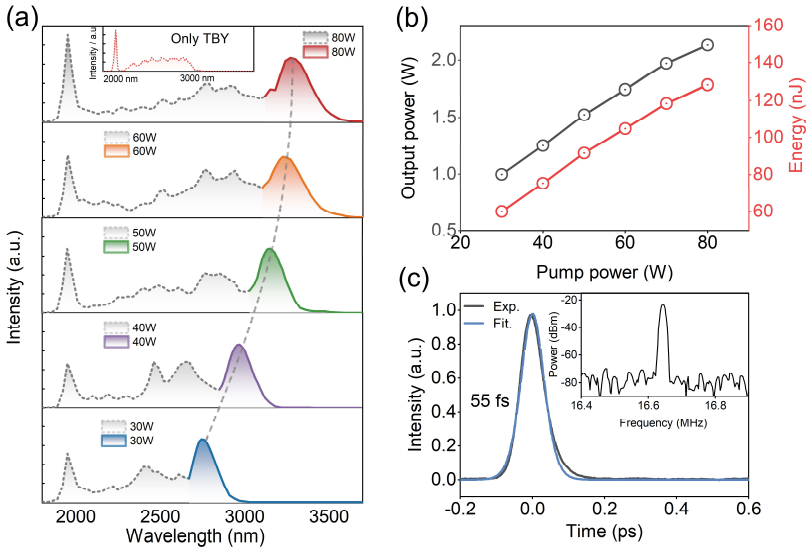

Figure 4. (a) Variation of the frequency shift spectrum of the Raman soliton in fluorotellurite fiber at 30W- 80W pump power (the inset shows the output spectrum at 8.5 W by directly pumping TBY); (b) Variation of the Raman soliton output power and energy with pump power; (c) Autocorrelation curves of the Raman soliton at 3.3 μm.

The combination of LMA silica fiber and LMA TBY fiber provides a significant enhancement in the output power and peak power of the MIR Raman soliton as shown in Figure 4(b). At a pump power of 30 W, the output power of the Raman soliton reaches 1 W, with a pulse energy of 60 nJ, surpassing the highest energy typically obtained in conventional fluoride fibers. As the pump power is further increased to 80 W, both the output power and energy of the Raman soliton are doubled to 2.1 W and 128 nJ, respectively, which represent the highest

https://doi.org/10.1017/hpl.2025.10042 Published online by Cambridge University Press

levels for output power and energy in the >3 μm wavelength range. Furthermore, using a 3 μm long-pass filter to isolate the Raman soliton at 3.3 μm, The radio-frequency (RF) spectrum of the Raman soliton was first measured using a spectrum analyzer, as shown in the inset of Figure 4(c). The signal-to-noise ratio (SNR) is approximately 51 dB, indicating that the 3.3 μm Raman soliton has good short-term stability. Moreover, the autocorrelation curve was measured using an autocorrelator, as shown in Figure 4(c). The pulsewidth is approximately 55 fs (corresponding to a peak power of 2.3 MW), which benefits from the ultra-short length of the TBY fiber, preventing pulse broadening due to fiber length and long-wavelength dispersion. Similar to the autocorrelation trace shown in Figure 3(c), the Raman soliton at 3.3 μm exhibits a smooth autocorrelation profile without any visible pedestal or sidelobes. This is attributed to the dynamic balance between GVD and SPM during soliton propagation, as well as the intrapulse Raman scattering that shifts energy from higher (shorter wavelength) to lower (longer wavelength) frequencies. This process inherently reshapes the temporal pulse profile, and the localized energy transfer effectively suppresses or eliminates weak edge components that may otherwise form a pedestal.

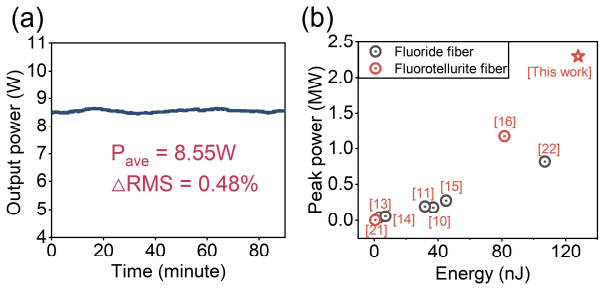

Figure 5. Evolution of the SC average power at 8.5 W over 90 minutes. ΔRMS refers to the normalized root mean square. (b) Summary of the literature on >3μm Raman soliton generation based on fluoride fiber and fluorotellurite fiber.

Finally, we monitored the power stability of the output laser, conducting a test for over 90 minutes at a maximum power of 8.5 W. As shown in Figure 5(a), the normalized root mean square (RMS) fluctuation is 0.48%, indicating minimal output power variation. Additionally, no power drop was observed during the 90 minutes monitoring period. We also compared the current performance of generating Raman solitons greater than 3 μm using fluoride fibers and fluorotellurite fibers. As shown in Figure 5(b), Raman solitons generated in fluoride fibers have limited pulse energies of below 50 nJ, with peak powers restricted to 0.5 MW. Although in our previous work, a new method involving gain control was used to increase the Raman soliton energy to 107 nJ, the output power was still limited to 100 mW, and the peak power did not reach the MW level. On the other hand, the work on generating Raman solitons with TBY fibers has not surpassed 100 nJ. In this study, we employed ultra-large core and ultra-short length TBY fiber as the nonlinear frequency-shifting medium, significantly enhancing the pulse energy of the Raman soliton and reducing its pulsewidth. The peak power has doubled

https://doi.org/10.1017/hpl.2025.10042 Published online by Cambridge University Press

compared to the highest level in previous studies, with energy and power breaking through 120 nJ and 2 W, respectively. Undoubtedly, our work has once again set a new record for the output parameters of MIR Raman solitons.

4. Theoretical study

To more clearly and intuitively observe the 1960 nm femtosecond laser's transmission process through the silica and TBY fibers, we solved the generalized nonlinear Schrödinger equation in MATLAB to obtain the temporal and spectral evolution at a pump power of 80 W. First, the initial input pulse parameters and the fiber lengths used in each section were set to match the experimental conditions, where the repetition frequency is 16.64 MHz, input power is 10.31 W, and pulsewidth is 460 fs. The total fiber length in the simulation was 0.37 m, with 0.27 m silica fiber and 0.10 m TBY fiber. For the fiber parameters, we imported the loss, dispersion, and mode field diameter as a function of wavelength for the silica fiber and 40 μm fluoride fibers in the simulation to ensure accuracy. As shown in Figure 6(a), the femtosecond pulse first undergoes self-compression in the silica fiber. Under the influence of SPM, the spectral width of the pulse rapidly expands, and the temporal pulse narrows. At approximately 0.05 m, the spectrum reaches its widest point, and the pulsewidth is compressed to its narrowest. Then the first-order Raman soliton begins to split, the frequency shift reaches approximately 2300 nm at 0.27 m, which is in close agreement with the experimental results.

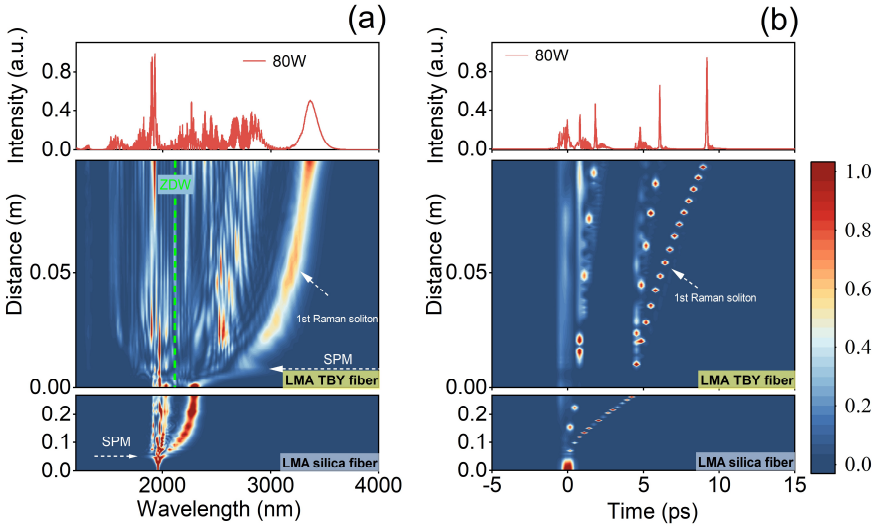

Figure 6. (a) Frequency-domain evolution and (b) time-domain evolution in the tapered TBY fiber at a pump power of 80 W.

Subsequently, the residual pump laser and the generated Raman soliton were coupled into the LMA TBY fiber with an efficiency of 84%. When the Raman soliton enters the 0.1 m LMA TBY fiber, due to its strong nonlinearity and the high peak power characteristics of the pump source, the Raman soliton (from silica fiber) further undergoes strong SPM as a higher-order soliton. During the period from 0.27 m to 0.278 m, the frequency domain undergoes significant broadening, and the pulse in the time domain is compressed. At 0.278 m, the first-order Raman

https://doi.org/10.1017/hpl.2025.10042 Published online by Cambridge University Press

soliton is re-generated and shifts to long wavelength region with a gradually decreasing speed. This is mainly attributed to the reduced nonlinear coefficient of the TBY fiber at longer wavelengths. At the end of the 10 cm 40 μm TBY fiber, the Raman soliton can shift to 3320 nm. In the entire frequency domain evolution diagram, the residual pump pulse in the silica fiber undergoes SPM after entering the normal dispersion region of the TBY fiber, with only a small portion of the laser shifting beyond the zero-dispersion wavelength.

Furthermore, we simulated the FROG and spectral phase of the Raman soliton centered at 3.32 μm. As shown in Figure 7 (a), the Raman soliton at the farthest wavelength of 3.32 μm is an isolated pulse which indicates that its phase is synchronized and stable, so we can experimentally isolate it using a 3 μm long-pass filter. The spectral phase of the 3.32 μm Raman soliton, as shown in Figure 7(b), displays a nearly linear and monotonically decreasing profile. It remains smooth and free of abrupt fluctuations, indicating that the pulse contains only linear chirp, which would not introduce a noticeable pedestal in the time domain.

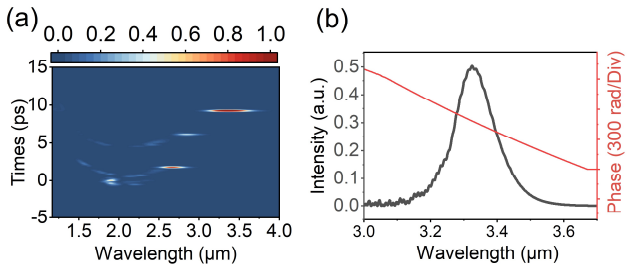

Figure 7. (a) Simulated FROG trace at the output end of the TBY fiber; (b) the spectral phase distribution of the Raman soliton centered at 3.32 μm.

5. Conclusion

In summary, we have achieved Raman solitons with a tuning range of approximately 600 nm for the first time in custom-made 10 centimeters mid-infrared fibers (TBY), with the furthest tuning wavelength reaching 3.3 μm. The overall technical approach employs a novel Raman soliton cascading method. A high-peak-power Raman soliton is first generated in silica fiber using a few-hundred-femtosecond 2 μm pulse, which serves as another pump source of the highly nonlinear TBY fiber. Due to the fiber's ultra-short length and ultra-large core features, the newly split Raman soliton undergoes minimal dispersion broadening during its frequency shift in the TBY fiber. Finally, the Raman soliton obtained at 3.3 μm has an extremely high peak power (2.3 MW), along with high output power (2.1 W) and pulse energy (128 nJ). Our technical approach will effectively enhance the output performance of MIR fiber lasers, with profound implications for applications such as high-order harmonic generation, high-resolution molecular spectroscopy, and imaging.

Acknowledgment

https://doi.org/10.1017/hpl.2025.10042 Published online by Cambridge University Press

This work was supported in part by the National Natural Science Foundation of China under Grants 62005004 and 61675009, and in part by the Natural Science Foundation of Beijing Municipality under Grants 4204091 and KZ201910005006, and in part by China Postdoctoral Science Foundation under Grants 212423.

References

1. S. Ghimire, A. D. DiChiara, E. Sistrunk, P. Agostini, L. F. DiMauro, and D. A. Reis, "Observation of high-order harmonic generation in a bulk crystal," Nat. Phys. 7, 138 (2011). DOI: https://doi.org/10.1038/nphys1847

2. G. Vampa, T. J. Hammond, M. Taucer, X. Ding, X. Ropagnol, T. Ozaki, S. Delprat, M. Chaker, N. Thiré, B. E. Schmidt, F. Légaré, D. D. Klug, A. Y. Naumov, D. M. Villeneuve, A. Staudte, and P. B. Corkum, "Strong-field optoelectronics in solids," Nat. Photonics 12, 465 (2018). DOI: https://doi.org/10.1038/s41566-018-0193-5

3. X. Wang, H. Yu, P. Li, Y. Zhang, Y. Wen, Y. Qiu, Z. Liu, Y. Li, and L. Liu, "Femtosecond laser-based processing methods and their applications in optical device manufacturing: A review," Opt. Laser Technol. 135, 106687 (2021). DOI: https://doi.org/10.1016/j.optlastec.2020.106687

4. R. F. Haglund Jr, N. L. Dygert, S. L. Johnson, K. E. Schriver, and H. K. Park, "Processing of polymer and organic materials by tunable, ultrafast mid-infrared lasers," *in Pacific International Conference on Applications of Lasers and Optics*, (Laser Institute of America, USA, 2008), p. 658-663.

5. K. C. Hartig, J. Colgan, D. P. Kilcrease, J. E. Barefield, and I. Jovanovic, "Laser-induced breakdown spectroscopy using mid-infrared femtosecond pulses," J. Appl. Phys. 118, 043107 (2015). DOI: https://doi.org/10.2351/1.5057099

6. J. Haas, B. Mizaikoff, "Advances in mid-infrared spectroscopy for chemical analysis," Annu. Rev. Anal. Chem. 9, 45 (2016). https://doi.org/10.1146/annurev-anchem-071015-041507

7. R. W. Waynant, I. K. Ilev, and I. Gannot, "Mid-infrared laser applications in medicine and biology," Philosophical Transactions of the Royal Society of London. Series A: Mathematical, Physical and Engineering Sciences 359, 635 (2001). DOI: https://doi.org/10.1098/rsta.2000.0747

8. J. P. Gordon, "Theory of the soliton self-frequency shift," Opt. Lett. 11, 662 (1986). DOI: https://doi.org/10.1364/OL.11.000662

9. F. M. Mitschke, L. F. Mollenauer, "Discovery of the soliton self-frequency shift," Opt. Lett. 11, 659 (1986). DOI: https://doi.org/10.1364/OL.11.000659

10. S. Duval, J. C. Gauthier, L. R. Robichaud, P. Paradis, M. Olivier, V. Fortin, M. Bernier, M. Piché, and R. Vallée, "Watt-level fiber-based femtosecond laser source tunable from 2.8 to 3.6 μm," Opt. Lett. 41, 5294 (2016). DOI: https://doi.org/10.1364/OL.41.005294

11. L. Yu, J. Liang, S. Huang, J. Wang, J.Wang, X. Luo, P. Yan, F. Dong, X. Liu, Q. Lue, C. Guo, and S. Ruan, "Generation of single solitons tunable from 3 to 3.8 μm in cascaded Er^{3+}-doped and Dy^{3+}-doped fluoride fiber amplifiers," Photonics Res. 10, 2140 (2022). DOI: https://doi.org/10.1364/PRJ.463613

12. I. Tiliouine, G. Granger, Y. Leventoux, CE. Jimenez, J. Melek, V. Couderc, and S. Février, "Two-octave mid-infrared supercontinuum pumped by a 4.5 μm femtosecond fiber source," https://ieeexplore.ieee.org/abstract/document/9890133 (September 23, 2022)

13. N. Nagl, K. F. Mak, Q. Wang, V. Pervak, F. Krausz, and O. Pronin, "Efficient femtosecond mid-infrared generation based on a Cr: ZnS oscillator and step-index fluoride fibers," Opt. Lett. 44, 2390 (2019). DOI: https://doi.org/10.1364/OL.44.002390

14. H. Ren, K. Xia, J. Wang, S. Ge, T. Huang, P. Yang, P. Xu, S. Mo, M. Qiu, S. Bai, F. Chen, S. Dai, and Q. Nie, "The polarization-aided tunable high-power femtosecond Raman solitons generation from 1.96 to 3.1 μm in fibers cascaded system," Opt. Laser Technol. 150, 107934 (2022). DOI: https://doi.org/10.1016/j.optlastec.2022.107934

15. I. Tiliouine, H. Delahaye, G. Granger, Y. Leventoux, CE. Jimenez, V. Couderc, and S. Février, "Fiber-based source of 500 kW mid-infrared solitons," Opt. Lett. 46, 5890 (2021). DOI: https://doi.org/10.1364/OL.445235

16. L. Yang, C. Yao, X. Wang, X. Meng, G. Ren, X. Yang, J. Pan, and P. Li, "Mid-infrared enhanced Raman soliton generation in an erbium-doped ZBLAN with record energy and peak power," Opt. Express 32, 42466 (2024). DOI: https://doi.org/10.1364/OE.539594

17. C. Yao, C. He, Z. Jia, S. Wang, G. Qin, Y. Ohishi, and W. Qin, "Holmium-doped fluorotellurite microstructured fibers for 2.1 μm lasing," Opt. Lett. 40, 4695 (2015). DOI: https://doi.org/10.1364/OL.40.004695

18. C. Yao, Z. Jia, Z. Li, S. Jia, Z. Zhao, L. Zhang, Y. Feng, G. Qin, Y. Ohishi, and W. Qin, "High-power mid-infrared supercontinuum laser source using fluorotellurite fiber," Optica 5, 1264 (2018). DOI: https://doi.org/10.1364/OPTICA.5.001264

19. N. Li, F. Wang, C. Yao, Z. Jia, L. Zhang, Y. Feng, M. Hu, G. Qin, Y. Ohishi, and W. Qin, "Coherent supercontinuum generation from 1.4 to 4 μm in a tapered fluorotellurite

https://doi.org/10.1017/hpl.2025.10042 Published online by Cambridge University Press

microstructured fiber pumped by a 1980 nm femtosecond fiber laser," Appl. Phys. Lett. 110, 061102 (2017). DOI: https://doi.org/10.1063/1.4975678

20. Z. Li, N. Li, C. Yao, F. Wang, Z. Jia, F. Wang, G. Qin, Y. Ohishi, and W. Qin, "Tunable mid-infrared Raman soliton generation from 1.96 to 2.82 μm in an all-solid fluorotellurite fiber," AIP Adv. 8, 115001 (2018). DOI: https://doi.org/10.1063/1.5042137

21. P. Chang, H. Luo, Q. Wu, Y. Wang, and J. Li, "Tunable mid-infrared Raman soliton generation from 2.80 to 3.17 μm based on fluorotellurite fiber," IEEE Photonics Technol. Lett. 34, 1183 (2022). DOI: https://doi.org/10.1109/LPT.2022.3201024

22. L. Yang, C. Yao, X. Wang, X. Meng, G. Ren, L. Pu, K. Li, and P. Li, "Generation of a MW-class tunable Raman soliton up to 3.8 μm in a fluorotellurite fiber," Opt. Lett. 49, 6137 (2024). DOI: https://doi.org/10.1364/OL.538227

23. G. P. Agrawal, "Nonlinear Fiber Optics," *in Nonlinear Science at the Dawn of the 21st Century*, P. L. Christiansen, M. P. Sørensen, and A. C. Scott, eds. (Springer Berlin Heidelberg, Berlin, Heidelberg, 2000), Chap. 12.

24. L. Yang, X. Wang, C. Yao, Z. Xu, G. Ren, K. Li, and P. Li, "High-power tunable Raman soliton generation in large core diameter passive fibers via a precise fundamental-mode matching technique," Opt. Express 32, 4036 (2024). DOI: https://doi.org/10.1364/OE.506443